Evaluation Beamline (BL-11) for Soft X-Ray Optical Elements

Kazuo Sano,[*] Takashi Imazono,[**] Masafumi Jinno,[***] Hiroyuki Sasai,[***]
Yoshihisa Harada,[***] Naoji Moriya,[***] Masahiko Ishino,[**] Masato Koike[**]

Abstract

An evaluation system capable of measuring the wavelength and angler characteristics of the absolute reflectivity (or diffraction efficiency) of soft X-ray optical elements has been operating on a beamline (BL-11) of the AURORA, a superconducting compact storage ring, at the Synchrotron Radiation Center, Ritsumeikan University since 2000. An outstanding feature of this beamline is a wide wavelength range covering of 0.7 nm < λ < 25 nm. For that purpose this system incorporates two types of Monk-Gillieson monochromators. One is a conventional type equipped with three varied-line-spacing gratings, allowing a choice of two included angles. The other is a new type that employs a scanning mechanism based on surface normal rotation. The outline of the system, typical experimental data obtained in the course of over 7 years runs, and a coming installation of a new polarimeter are described.

[*] *Shimadzu Emit Co. Ltd., 2-5-23, Kitahama, Chuo, Osaka 541-0041, Japan*

[**] *Quantum Beam Science Directorate, Japan Atomic Energy Agency, 8-1, Umemidai, Kizugawa, Kyoto 619-0215, Japan,*

[***] *Shimadzu Corp., Kyoto 604-8511* [**] *Shimadzu Corp., Kyoto 604-8511*

1. INTRODUCTION

There has been a pressing need in the Japanese soft-x-ray (SXR) optics community for a dedicated evaluation facility capable of characterizing state-of-the-art SXR optical elements, such as advanced-type gratings, SXR multilayer-coated elements, polarizing elements, etc. To meet the needs we have designed evaluation beamline optics on the basis of a theory [1] specifically developed for the purpose and an end station for measuring optical characteristics of SXR optical elements. The use of a light source having high brightness with temporal and spatial stabilities is essential for SXR optical element evaluation systems. Therefore, we have installed a new evaluation system for SXR optical elements on a beamline (BL-11) of the AURORA, a superconducting compact storage ring [2], at the Synchrotron Radiation Center of Ritsumeikan University in Kusatsu, Shiga, Japan.

To cover a wavelength range of 0.5 nm < λ < 25 nm, two types of grazing incidence Monk-Gillieson monochromators are incorporated in the system; one is the conventional type and the other is a new type that employs a scanning mechanism based on surface normal rotation (SNR) of the grating. This scanning scheme was proposed by Hettrick [3] in 1992 on account of high grating efficiencies in conical diffraction (or extreme off-plane) mountings. The practical advantage of the scheme lies in its simplicity, requiring only a simple rotation of the grating about its normal.

We describe this unique beamline optics and give some preliminary data measured on a multilayer, diffraction gratings, and a filter, together with the results of crosscheck measurements of the same samples made on another facility. Also we introduce new apparatus for SXR polarimetry and ellipsometry which is under construction to accelerate the developments of new polarizing elements.

2. INSTRUMENTATION

The remarkable features of the AURORA are utilization of a single superconducting magnet and an exactly circular electron orbit. Thus, the AURORA maintains its electron beam and synchrotron radiation extremely stable. The major machine parameters are as follows: electron energy = 575 MeV; orbital radius = 1.0 m, critical wavelength λ_c = 1.5 nm; electron beam current = 300 mA; horizontal beam size σ_y = 1.3 mm; vertical beam size σ_z = 0.14 mm; brightness = 1.8×10^{12} photons/sec/mm^2/mrad^2/0.1%BW @4.5nm.

The evaluation beamline consists of four systems: (1) prefocus system, (2) monochromator system, (3) reflectometer system, and (4) control. The overall length of the beamline (the source point S-to-the end station GO) is about 10 m system (refer to Fig. 1 and Table 1).

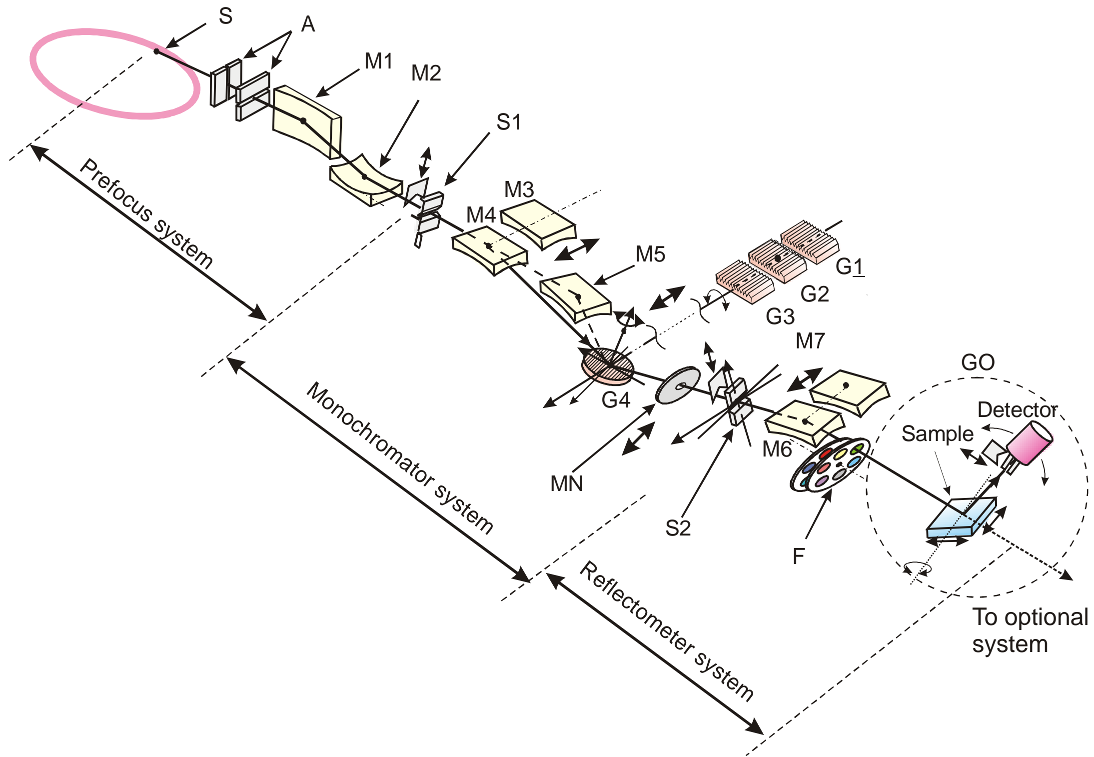

Fig.1. Schematic diagram of the evaluation beamline

The prefocus system comprises beam-shaping apertures, focusing mirrors, and filters. The light beam from the source point S goes through the front end and reaches to the two sets of mutually perpendicular beam-shaping apertures A. The maximum acceptance angles determined by the apertures are 5 mrad (H) × 3 mrad (V). Then, the light beam is focused on the entrance slit S1 horizontally by the spherical mirror M1 and vertically by the spherical mirror M2.

The monochromator system is the most unique component of the beamline and consists of two types of Monk-Gillieson monochromators. One is a conventional Monk-Gillieson monochromator equipped with three laminar-type varied-line-spacing holographic gratings [4] G1 (300 lines/mm), G2 (600 lines/mm), and G3 (1200 lines/mm). These gratings are used interchangeably at an included angle of either 176° or 172°[5], depending on a required scanning range. One particular included angle is easily selected by inserting the vertical focusing spherical mirror M3 or M5 into the beam at an angle of incidence of 88° or 86°. The various combinations of these gratings and mirrors make it possible to cover the wavelength region of 1.2 nm $< \lambda <$ 25 nm.

The other monochromator is a Monk-Gillieson monochromator that operates in the SNR scanning mode. In the SNR mode the vertical focusing spherical mirror M4 is inserted into the beam at an angle of incidence of 88° while keeping M3 and M5 out of the beam. The convergent beam reflected from M4 impinges on the surface of a conventional plane grating

Table 1. Optical parameters of the evaluation beamline.

	M1	M2	S1	M3	M4	M5	G1	G2	G3	G4	S2	M6
Distance from source(mm)	2400	3000	4200	6200	6200	6451	6700	6700	6700	6700	8200	9200
Distance from previous element (mm)	2400	600	1200	2000	2000	2251	500 or 251	500 or 251	500 or 251	500	1500	1000
Incidence angle (deg)	88	88	-	88	88	86	88 or 86	88 or 86	88 or 86	88	0	88
Shape	Spherical	Spherical	-	Spherical	Spherical	Spherical	Plane	Plane	Plane	Plane	-	Toroidal
Material	SC.Silicon	F.Silica	-	F.Silica	F.Silica	F.Silica	F.Silica	F.Silica	F.Silica	F.Silica	-	F.Silica
Raduis of curvature(W,mm)	58945	49121	-	57307	79647	28232	∞	∞	∞	∞	-	28654
Radious of curvature(H,mm)	-	-	-	-	-	-	-	-	-	-	-	58.0
CLS or VLS	-	-	-	-	-	-	VLS	VLS	VLS	CLS	-	-
Grating constant(l/mm)	-	-	-	-	-	-	300	600	1200	1200	-	-
Dimenstion W (mm)	400	300	-	200	200	150	100	100	100	120Phi	-	200
H(mm)	50	50	-	40	40	40	40	40	40	65	-	40
D(mm)	40	40	-	40	40	40	18	18	18	25	-	40
Coating Material	Au	Au	-	Au	Au	Au	Au	Au	Au	Au	-	Au

G4 (1200 llines/mm), which is used at an included angle of 176°. This SNR Monk-Gillieson monochromator covers a wavelength range of about 0.5–2 nm. The detail of the design of this monochromator is described in Ref. 1.

Figure 2 shows a schematic diagram of the mechanical system for the selection of one particular grating and wavelength scanning mode. The gratings G1, G2, and G3 are mounted in the rotatable holder E, which is driven by the wheel W. The grating G4 is fixed on the turntable T. E, W, and T move together as the slide F is translated by means of the screw R1 and guide rod R2 attached to the main frame MF. Thus, one particular grating can be easily brought into the incident beam by moving F. Wavelength scanning in the conventional mode is carried out by rotating E. Rotational motion of the driving rod RD is transmitted to E through W by means of a tensioned metal belt B. In the SNR mode, G4 is rotated by means of a pair of bevel gears driven directly by RD. This mechanism facilitates the selection of one particular grating and the associated scanning mode without breaking vacuum.

To monitor the flux stability and to aid optical alignment, an Au-mesh beam intensity monitor MN can be inserted between the gratings and the exit slit S2. The monochromatized beam emerging from S2 is focused onto a sample placed in the goniometer GO by the toroidal mirror M6.

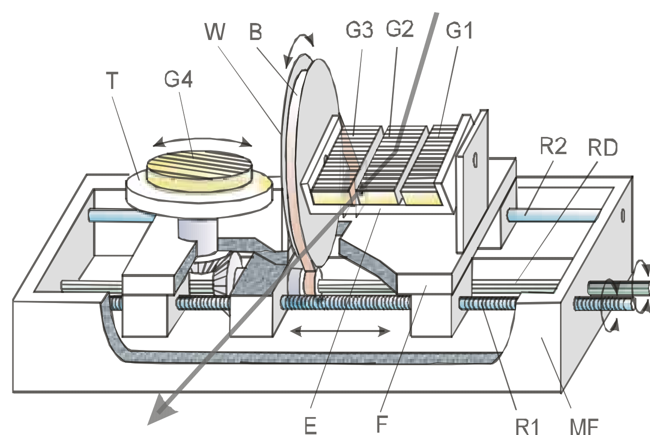

Fig. 2. Schematic diagram of the mechanical system for the selection of one particular grating and wavelength scanning mode.

Total distance from the source point to the sample is 10.2m.

Another toroidal mirror M7 can also be used when an end station is connected the GO chamber in tandem. This mirror M7 provides focus at a point 150 mm downstream from the back flange of the GO chamber. Tandem two filter-wheels F located in front of the reflectometer hold 2 × 5 filters in total. Currently, Ti, C, Cr, Si, Al, Fe, and Ni filters (nominal thickness of 0.5-μm) are set in each filter-wheel.

The reflectometer system consists of a modified θ-2θ reflectometer/diffractometer. The sample stage (θ-stage) of GO accommodates a sample of up to 254 mm × 254 mm, and the sample surface can be scanned by a spot of ~1 × 2 mm^2 by an *X-Y* sample translation mechanism. The reflected (or diffracted) beam from the sample is detected by a Si or GaAsP detector mounted on the 2θ-arm. The θ-stage and 2θ-arm can also be controlled independently when needed.

The control system controls all the functions incorporated in the evaluation system. The computer control system is operated by software written with LabVIEW® and running on a PC compatible computer. The task oriented software makes it possible to measure the reflectivities (or diffraction efficiencies) of the multilayer mirrors (or gratings) against wavelength or incident angle by controlling both the monochromator and the goniometer simultaneously.

3. PERFORMANCE

The performance of the evaluation system for SXR optical elements has been evaluated in the course of test run. This has been done by measuring the reflectivity of a Mo/Si multilayer at around 14 nm, the absolute efficiencies of spherical gratings in a range of 4-18 nm, and the transmittance of an Al filter at around 0.8 nm.

The measurements on the multilayer and gratings were made in the conventional Monk Gillieson monochromator mode with G1 (300 lines/mm) and M5 (included angle of 172°). The results were compared with the data obtained at the ALS using the standard and calibration beamline (BL 6.3.2) whose monochromator is of the conventional Monk-Gillieson type with a ruled master grating of 300 lines/mm at an included angle of 172° [6,7].

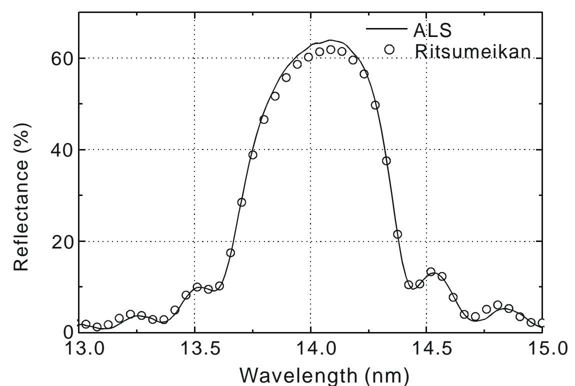

Fig. 3. Reflectance of a Mo/Si multilayer mirror at an angle of incidence of 5°.

The multilayer data thus obtained at the two facilities are compared in Fig. 3,

where the solid curve and the open circles indicate the data of the ALS and the Ritsumeikan, respectively. This shows the reflectivity of a Mo/Si-multilayer mirror measured at an angle of incidence of 5°. The mulitlayer used for the evaluation was deposited at NTT-AT and has a period of 6.39 nm, a value of 0.4 for Mo-layer thickness/period, and 40 layer pairs. To suppress the effect of overlapping higher orders, a Si filter was used at the both facilities and a 3-mirror reflector [7] was also used at the ALS. It is clearly seen in the figure that both the data taken independently coincide with each other.

The absolute diffraction efficiencies were measured on a laminar-type master holographic grating (HG) [8,9] and two commercial replica gratings (RG1 and RG2) replicated from one and the same ruled VLS master grating [10]. Both the holographic and ruled gratings were for the SXR flat-field spectrograph developed by Harada and Kita.[10] HG and RG1 were measured at the Ritsumeikan and HG and RG2 at the ALS. These gratings are all Au-coated and have a effective groove density of 1200 lines/mm. HG has a radius of curvature of 5409 mm, a groove depth of 10nm, and a duty ratio (ratio of the land-width to the period) of 0.32 measured at its center. Both RG1 and RG2 have a radius of curvature of 5649 mm and a blaze angle of 3.2°, which gives a blaze wavelength of 10 nm at an angle of incidence of 87º. The measurements were performed at a fixed angle of incidence of 87º over a range of ~4–18 nm so as to conform to the design of the flat-field spectrograph [10].

Figures 4(a) and 4(b) show the absolute diffraction efficiency curves measured on HG and those on RG1 and RG2, respectively. The solid lines with the letter R indicate the data obtained at the Ritsumeikan and the dotted lines with A show those at the ALS. In the figure, *m* is the spectral order. The efficiencies of the holographic grating HG measured at the two

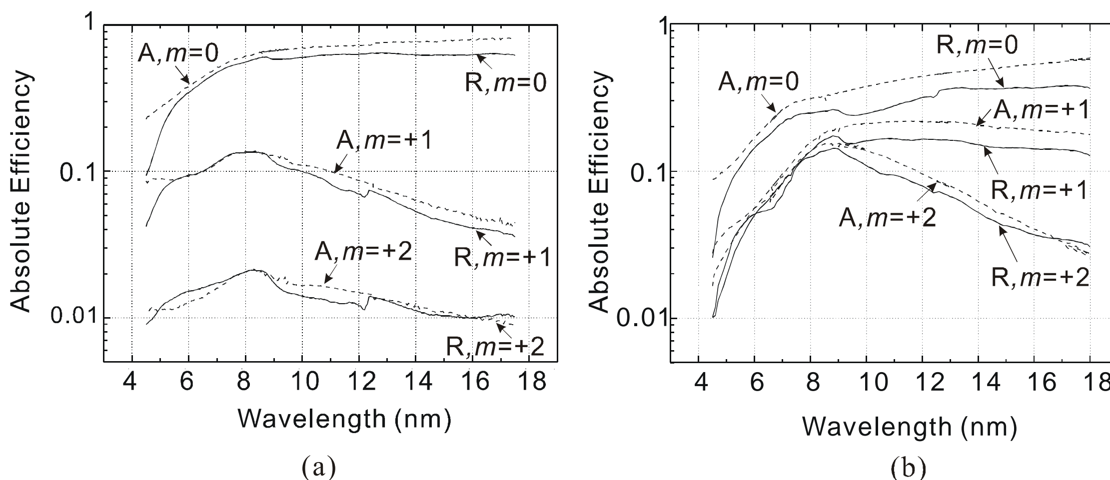

Fig. 4. Absolute diffraction efficiencies of HG (a) and those of RG1 and RG2 (b). The solid lines with the letter R indicate the data obtained at the Ritsumeikan and the dotted lines with A show those at the ALS, and *m* is the spectral order.

facilities well coincide with each other. However, the efficiency curves of RG1 and those of RG2 showed relatively larger discrepancies, especially at wavelengths 10–18 nm. The reason for this is not clear at present, except that the same replica grating was not measured at the two facilities.

The performance of the evaluation system in the SNR mode was examined by measuring the transmittance of a commercial Al filter (nominal thickness of 0.5-μm) at around the Al K-edge (0.795 nm). Figure 5(a) shows the measured data. The solid and dotted lines show the transmitted intensities I and the reference intensities I_0 measured without the filter, respectively. Besides the Al K-edge, a small Si K-edge absorption is observed in both the I_0 and I curves at around 0.674 nm. By contrast, similar measurements made in the conventional Monk-Gillieson monochromator mode failed to produce meaningful data on the Al filter because of low efficiencies of the gratings at these short wavelengths that resulted in a lack of sufficient I_0 and in a high noise level. This furnishes a proof that the grating efficiency in the SNR mode is much higher than that in the conventional mode. Thus, the SNR Monk-Gillieson monochromator would play a key role in bridging the gap between the grating monochromator and the crystal monochromator in the energy region of 1–2 keV and in attaining high flux and high resolution when used with a third-generation synchrotron radiation source.

In Fig. 5(b), the solid line shows the transmittance curve reduced from the measured data of Fig. 5(a). This curve is compared with those calculated on Web[11] The transmission

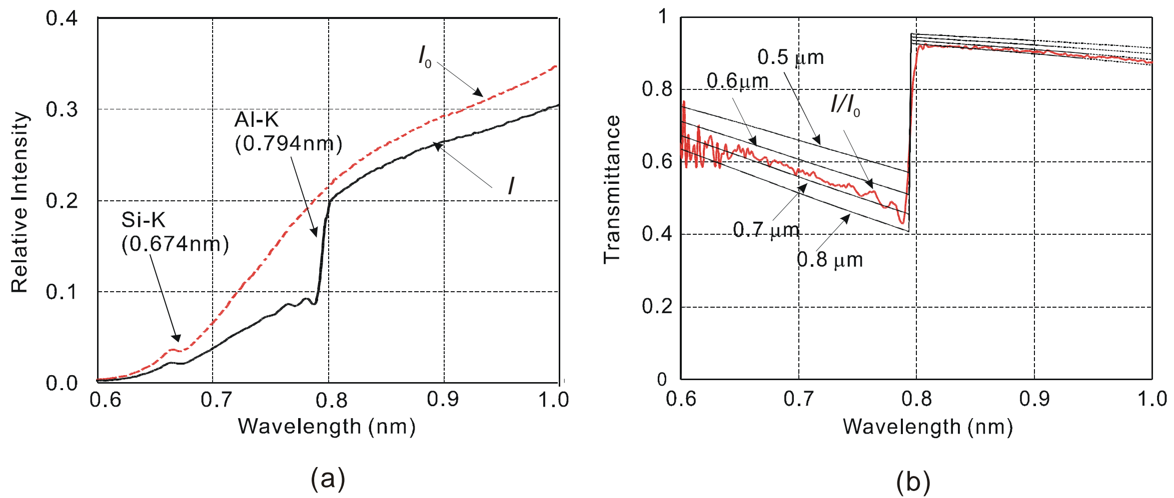

Fig. 5. Transmittance of an Al filter (nominal thickness of 0.5-mm) measured by the SNR Monk-Gillieson monochromator. (a) The transmitted intensity I (solid line) and reference intensity I0 (dotted line) and (b) transmittance curve reduced from the measured data (solid line) and those calculated on Web [11] assuming films of 0.5, 0.6, 0.7, and 0.8-mm thick (dotted line).

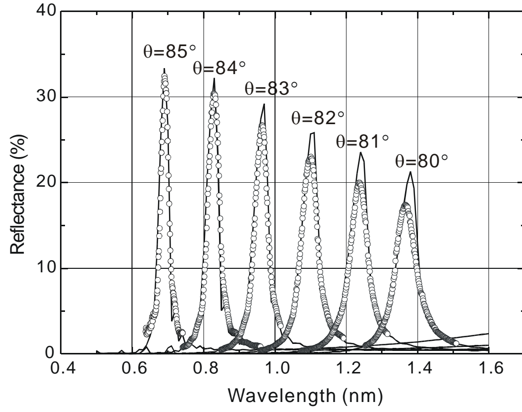

Fig.6. Reflectance of a Pt/C multilayer at angles of incidence of θ= 80°, 81°, 82°, 83°, 84°, and 85°. The open circles and the solid curves indicate the data of the measured and theoretical reflectance assuming a surface roughness of 0.43 nmRMS, respectively

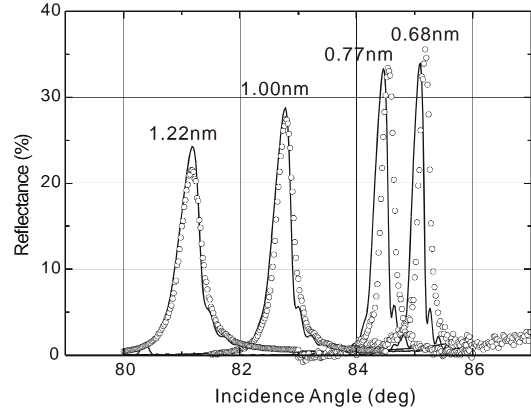

Fig.7. Reflectance of a Pt/C multilayer at wavelengths of 0.68, 0.77, 1.00, and 1.22 nm. The open circles and the solid curves indicate the data of the measured and theoretical reflectance assuming a surface roughness of 0.43 nmRMS, respectively.

curves calculated for films of 0.5, 0.6, 0.7, and 0.8-μm thick are indicated by dotted lines. The measured curve agrees well with the calculated curve for a film of 0.7-μm thick, again supporting the reliability and the usefulness of the SNR Monk-Gillieson monochromator

The wavelength and angular characteristics of a Pt/C multilayer mirror were measured by use of the SNR monochromator in the 0.7−1.5 nm region. The reflectance measured at angles of incidence of 80°, 81°, 82°, 83°, 84°, and 85° are shown in Fig. 6, where the open circles and the solid curves indicate the data of the measured and theoretical reflectance assuming a surface roughness of 0.43 nmRMS, respectively. The mulitlayer used for the evaluation was deposited at Nagoya Univ. and has a period of 1.78 nm, a value of 0.37 for Pt-layer thickness/period, and 30 layer pairs. It is clearly seen in the figure that the peak wavelengths depending on the angle of incidence agree with those are expected by the simulation.

Fig. 7 shows the reflectance of same Pt/C multilayer mirror measured at wavelengths of 0.68, 0.77, 1.00, and 1.22 nm. The open circles and the solid curves indicate the data of the measured and theoretical reflectance assuming a surface roughness of 0.43 nmRMS, respectively.

All the data presented above support the reliability of the evaluation system installed at the BL-11 at the Synchrotron Radiation Center, Ritsumeikan University and also the advantage of the SNR Monk-Gillieson monochromator at short wavelengths.

4. POLARIMETRY AND ELLIPSOMETRY–COMING IMPROVEMENT

Polarized light of a wavelength of 0.5-2.0 nm is useful for magnetic material sciences, e.g., magnetic circular dichroism spectroscopy. In such studies, it is important to obtain the information on the actual polarization state of the incident beam using as the probe light. In order to determine the polarization characteristics of light, polarizing elements such as polarizers and phase shifters are indispensable, so that we have made a start on developing soft x-ray polarizing elements working in the wavelength of 0.5-2.0 nm.[12, 13]

The performance of a reflection-type polarizer can be evaluated by measuring both reflectances for s- and p-polarization. According to dynamical theory of x-ray diffraction, the reflectance for p-polarization can be expected to be significantly low at the incident angle of 45° compared to that for s-polarization. Before the detailed evaluation of the polarization performance of the polarizer, it is beneficial to measure only the reflectance for s-polarization in advance. The preliminary reflection measurement of muscovite mica was carried out by means of the evaluation system for SXR optical elements in the conventional Monk-Gillieson monochrometor mode with G3 (1200 lines/mm) and M3 (included angle of 176°), where muscovite mica is well-known as a good dispersive optical element for x-ray region and has a *d*-spacing of about 1 nm suitable for a polarizer for a wavelength of 1.4 nm. The energy resolving power was estimated to be approximately 100 at 1.4 nm.

Figure 8 shows the measured reflectance for s-polarization of muscovite mica(002) in the symmetric Bragg case at a wavelength of 1.39 nm. The peak reflectance is evaluated to be about 1.3% at around 45° incidence. The solid line means the simulated curve based on dynamical theory of x-ray diffraction. The absolute value and width of measured data disagree with those of calculated curve. This can be explained by considering the monochromaticity and the divergence of the incident beam.[12] The result of the preliminary experiment indicates that muscovite mica has a possibility to work as a reflection-type polarizer for around 1.4 nm.

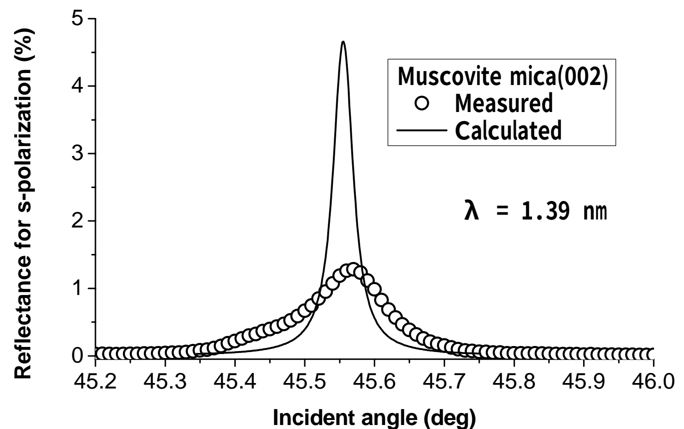

Fig.8 Measured reflectance for s-polarization of muscovite mica(002) in the symmetric Bragg case at 1.39 nm, as a function of the incident angle. Solid line indicates calculated curve based on dynamical theory of x-ray diffraction. The polarizing ability of a crystal-type polarizer becomes high at the incident angle of 45°.

Figure 9 shows measured reflectances for s-polarization of synthetic mica(002) in the symmetric Bragg case at the incident angle of around 45° as a function of the incident energy, where synthetic mica, fluoroflogopite, has a *d*-spacing of 0.9963 nm and lots of similar properties to muscovite mica. The peak reflectance at every incident angle indicated in the figure was evaluated to be over 1.2%. This result means that synthetic mica is also a promising candidate as a reflection-type polarizer although the reflectance for p-polarization is needed to measure under the same experimental condition.

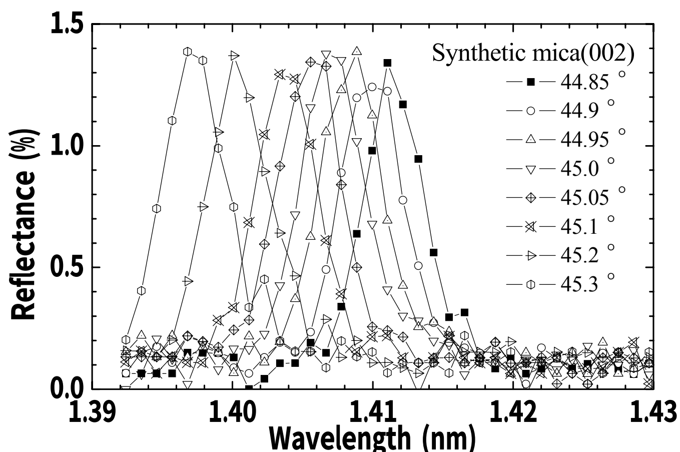

Fig.9 Measured reflectances for s-polarization of synthetic mica(002) at the fixed angles of incidence that are indicated in this figure, as a function of the incident energy.

The detailed polarimetrical measurements of both muscovite and synthetic micas were carried out at the BL23SU beamline of the SPring-8 and summarized in Table 2.[13] The polarizance (Γ) is defined as $(R_s - R_p)/(R_s + R_p)$, where R_s and R_p mean the reflectances for s- and p-polarization, respectively. The degree of linear polarization of light was determined simultaneously when the polarizance of the polarizer was evaluated. Muscovite and synthetic micas were found out to work the reflection-type polarizers for 1.4 nm having highly polarizing abilities. Also, by using them, the degrees of linear polarization of light in horizontal polarization mode were experimentally determined to be 99.3% at a wavelength of 1.4 nm for the first time and they agreed with each other.

To facilitate the developments of new soft X-ray polarizing elements it is indispensable to equip the capabilities of whole polarimetrical measurements at the evaluation system at the BL-11. From this standpoint a supplemental apparatus for polarimetry and ellipsometry having 8-axis goniometer has been designed and is currently under construction. This apparatus will be installed at the downstream of the existing goniometer (refer to Fig.10) in the fall of 2007. It allows us to characterize new polarizing elements such as multilayer- and crystal-types ones and determine the complete polarization state of light described by Stokes

Table 2 Polarization abilities, the reflectances for s- and p-polarization and the polarizance, of polarizers made with muscovite and fluorophlogopite micas.

	R_s	R_p	Γ
Muscovite	3.0%	0.015%	99.0%
Fluorophlogopite	2.6%	0.013%	99.9%

parameters. The 8-axis goniometer equipped in this apparatus has two stages to mount polarizing elements and employ a multi-channel plate (MCP) detector. One is used for a polarizer/phase shifter (P) at a pre-stage and the other for an analyzer (A) at a post-stage. The rotating-analyzer assembly consists of the analyzer at the post-stage and the MCP detector just behind the analyzer. This apparatus makes it possible to realize four scanning modes, which are double-reflections (transmissions), i.e., both P and A are reflection- (transmission-) types, transmission-reflection, i.e., P is transmission-type and A, reflection, and reflection-transmission, i.e., P is reflection-type and A, transmission. All axes can be driven with HV compatible internal stepping motors. This apparatus will be utilized for developing new polarizing elements not only for the wavelength region of 0.5-2.0 nm but also for the whole region which the BL-11 beamline covers and their applications to determination of the complete polarization state of light.

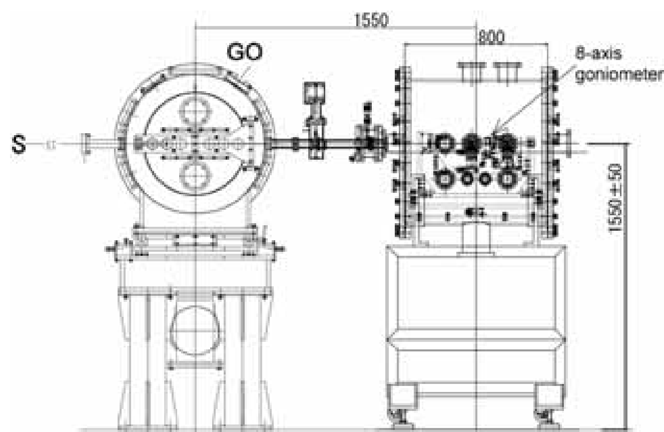

Fig. 10 Schematic of the new apparatus for SXR polarimetry and ellipsometry (right-hand side) linked to the evaluation system for SXR optical elements (left-hand side).

Acknowledgement

The authors are grateful to Dr. E. M. Gullikson at Center for X-ray Optics, Lawrence Berkeley National Laboratory, for his measurements at the ALS beamline 6.3.2, and Dr. K. Tamura and Prof. K. Yamashita at Nagoya University, Dr. H. Takenaka, NTT Advanced Technology Co., for providing their multilayer samples, and Itoh Kikoh Co., Ltd., Tokai, Aichi, Japan for providing their synthetic mica samples. They would also like to thank Prof. Dr. T. Namioka of Tohoku University, Dr. H. Kimura of JASRI/SPring-8, and Dr. Y. Saitoh of JAEA for their fruitful discussion.

The work done at the ALS was partly supported by the Director, Office of Energy Research, Office of Basic Energy Sciences, Materials Science Division, of the Department of Energy under contract No. DE-AC03-76SF00098. The experiment performed at SPring-8 was performed under the approval of the Japan Synchrotron Radiation Research Institute (JASRI) (Proposal No.2004B0748).

References

[1] M. Koike and T. Namioka, Appl. Opt., **41**,245 (2002).

[2] H. Iwasaki, Y. Nakayama, K. Ozutsumi, Y. Yamamoto, Y. Tokunaga, H. Saisho, T. Matsubara, and S. Ikeda, J. Synchrotron Rad. **5**, 1162 (1998).

[3] M. C. Hettrick, Appl. Opt. **31,** 7174 (1992).

[4] M. Koike and T. Namioka, Appl. Opt. **36**, 6308 (1997).

[5] M. Koike and T. Namioka, J. Electron Spectroscopy and Related Phenomena, **80**, 303 (1996).

[6] M. Koike, R. Beguiristain, J. H. Underwood, and T. Namioka, Nucl. Instr. Methods, **A347**, 273 (1994).

[7] J. H. Underwood, E. M. Gullikson, M. Koike, P. J. Batson, Proc. SPIE, **3113**, 214 (1997).

[8] M. Koike, T. Yamazaki, and Y. Harada, J. Electron Spectroscopy and Related Phenomena, **101-103**, 913 (1999).

[9] M. Koike, T. Namioka, E. Gullikson, Y. Haradad, S. Ishikawab, T. Imazono, S. Mrowka, N. Miyata, M. Yanagihara, J. H. Underwood, K. Sano, N. Ogiwara, O. Yoda, and S. Nagai, Proc. SPIE, **4146**,163 (2000).

[10] T. Kita, T. Harada, N. Nakano, and H. Kuroda, Appl. Opt. **22**, 512 (1983).

[11] http://cindy.lbl.gov/optical_constants/filter2.html.

[12] T. Imazono, M. Ishino, M. Koike, H. Kimura, T. Hirono, and K. Sano, Rev. Sci. Instrum., **76**, 023104 (2005).

[13] T. Imazono, T. Hirono, H. Kimura, Y. Saitoh, M. Ishino, Y. Muramatsu, M. Koike, and K. Sano, Rev. Sci. Instrum., **76**, 126106 (2005).